

## Sigma Stellation: A Design Strategy for Electron Boxes

Karl K. Irikura<sup>†</sup>

Computational Chemistry Group, National Institute of Standards and Technology,  
Gaithersburg, Maryland 20899-8380

Received: October 26, 2007

The carbon–fluorine antibonding ( $\sigma^*$ ) orbitals in a fluorocarbon cage are directed toward a central, common point. If the cage is not too large or too small, then the  $\sigma^*$  orbitals will overlap at that point. An added electron can occupy the resulting molecular orbital, suggesting that cage perfluorocarbons will have large electron affinities. This prediction is supported by electronic structure calculations of all of the fluorinated derivatives of tetrahedrane, cyclopropane, and cubane and of some other fluorinated cage and ring compounds. Perfluorododecahedrane ( $C_{20}F_{20}$ ) is predicted to have an electron affinity of about 3.4 eV, which is equal to that of the fluorine atom. A few speculative extensions and applications are suggested.

### Introduction

Fluorine is the most electronegative element, but fluorocarbon molecules do not have particularly large electron affinities. For example,  $CF_4$  and  $C_2F_6$  do not bind an additional electron at all.<sup>1–3</sup> Although this may be surprising initially, it may be understood as a *consequence* of the high electronegativity of fluorine, which results in strongly polar C–F bonding. That is, the C–F bonding orbital ( $\sigma$ ) is dominated by fluorine, which means that the corresponding C–F antibonding orbital ( $\sigma^*$ ) must be dominated by carbon. An added electron must enter the  $\sigma^*$  orbital, which reflects the properties of carbon more than those of fluorine. Another way to describe the situation is that the C–F bonds are partly ionic. Because the fluorine atoms already have significant negative charge, they are not attractive to an additional electron.

This molecular orbital description rationalizes why the high electronegativity of fluorine does not bestow fluorocarbons with high electron affinities. It does not explain why the electron affinities should be even lower than that of the carbon atom,<sup>4</sup> 1.26 eV (1 eV  $\approx$  96.5 kJ mol<sup>-1</sup>), despite the substantial ionic character of the C–F bond. To rationalize this observation, note that the C–F  $\sigma^*$  orbital resembles a carbon  $sp^3$  hybrid orbital. An electron in this orbital will be repelled from the internuclear (C–F) region by the electrons in the C–F  $\sigma$  orbital. It will tend to occupy the lobe of the orbital directed away from the fluorine atom. In many molecules, this location is crowded by other, destabilizing electron pairs. For example, in  $CF_4$  each  $\sigma^*$  orbital is crowded by fluorine lone pairs, which will repel an added electron. In contrast, tertiary C–F centers are less encumbered and react more readily in many contexts.<sup>1,3,5–9</sup>

If empty  $\sigma^*$  orbitals are arranged in space so that they overlap, then the lowest of the resulting unoccupied molecular orbitals will be delocalized and may be expected to show unusual stability. This is illustrated in Scheme 1. The present investigation tests the prediction that such starlike arrangements of  $\sigma^*$  orbitals will lead to high electron affinities.

### Computational Methods

The B3LYP/6-31+G(d)//HF/6-31+G(d) procedure was used for determining adiabatic electron affinities. Neutral and anionic geometries were optimized independently at the uncorrelated HF/6-31+G(d) level. Calculations on the radical anions were spin-unrestricted. Linear dependencies in the basis set were removed by deleting one or more basis functions according to the default criterion. Harmonic vibrational zero-point energies (ZPEs) were also computed at this level and scaled by 0.9153 as recommended.<sup>10</sup> Electronic energies were then computed using the hybrid density functional B3LYP<sup>11–13</sup> at the HF geometries. ZPEs were added to these electronic energies to obtain ground-state molecular energies. The adiabatic electron affinity (EA) is defined as the difference between the energies of the neutral and anionic ground-state molecules,  $EA = (E_{\text{neutral}} - E_{\text{anion}})$ . For the radical anions, the values of  $\langle S^2 \rangle$  are all  $\leq 0.77$ ; spin contamination was not a problem. The Gaussian software was used for the electronic structure calculations.<sup>14–16</sup>

In Table 1, the present B3LYP/HF results are compared with the corresponding experimental adiabatic electronic affinities for a set of molecules taken from recent compilations.<sup>17–19</sup> When comparing a theoretical method with experimental benchmark values, a small standard deviation indicates that the method is reliable for trends. If, in addition, the mean value is close to zero, then the method is also quantitatively reliable. Thus, the B3LYP procedure appears to overestimate EA by about 0.33 eV but to give relative values within about 0.14 eV ( $1\sigma$ ). Note that the molecules in the test set are more dissimilar than the hydrofluorocarbons of interest, so relative values in homologous series are probably more reliable than suggested by the results in Table 1.

### Results

Molecular symmetries, scaled ZPEs, B3LYP/HF electronic energies, and the corresponding adiabatic electron affinities are compiled in Table 2 for selected molecules. In many cases, included in the Supporting Information (Table S2) but usually not in Table 2, the calculated electron affinity is negative. This means that the molecule does not bind an electron, so the correct EA = 0. Despite being unbound, the calculations on the anions

<sup>†</sup> Author to whom correspondence should be addressed. E-mail: karl.irikura@nist.gov.

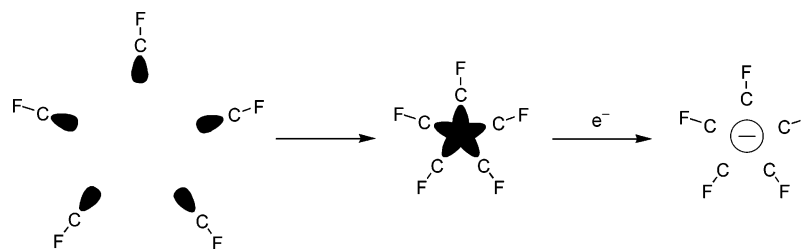
SCHEME 1: Unusually Stable LUMO from Starlike Arrangement of  $\sigma^*$  Orbitals

TABLE 1: Performance of Theoretical Procedures for Adiabatic Electron Affinities (eV)

molecule	expt.	B3LYP//HF error <sup>a</sup>
HNO	0.338 ± 0.015 <sup>19</sup>	0.39
<i>t</i> -dicyanoethylene	1.249 ± 0.087 <sup>19</sup>	0.37
maleic anhydride	1.44 ± 0.09 <sup>19</sup>	0.36
anthracene	0.530 ± 0.005 <sup>19</sup>	0.21
tetracyanoethylene	3.17 ± 0.2 <sup>19</sup>	0.45
cyclooctatetraene	0.55 ± 0.02 <sup>19</sup>	0.35
<i>p</i> -benzoquinone	1.860 ± 0.005 <sup>19</sup>	0.42
azulene	0.757 ± 0.005 <sup>17</sup>	-0.01
nitrobenzene	1.00 ± 0.01 <sup>17</sup>	0.45
nitromethane	0.26 ± 0.08 <sup>17</sup>	0.30
mean		0.33
standard deviation		0.14

<sup>a</sup> Errors are relative to experimental values.

proceed normally because the basis set confines the added electron artificially. The negative EA values are useful within the computational model for determining trends and substituent effects. The computations, however, are not suitable for predicting resonances,<sup>20</sup> so the present values should not be interpreted as such.

The computed EA values for the fluorinated methanes, CH<sub>4-n</sub>F<sub>n</sub>, are plotted in Figure 1. None is positive-valued. Increased fluorination raises the calculated EA only slightly, with smaller increases as more fluorine atoms crowd the carbon center. The situation is different for the tetrahedranes, C<sub>4</sub>H<sub>4-n</sub>F<sub>n</sub>. The first two fluorines have little effect, but the third and fourth increase the EA substantially (Figure 1). Nonetheless, only the perfluorinated compound has a positive value, and even that value is smaller than the overestimate suggested by Table 1. The spin density in the perfluorotetrahedrane radical anion, shown in Figure 2, supports the qualitative model depicted in Scheme 1. Analogous results for the fluorinated cyclopropanes, C<sub>3</sub>H<sub>6-n</sub>F<sub>n</sub>, are also shown in Figure 1. For *n* = 2, 3, and 4, there are three isomers. The isomer with the highest (i.e., most positive) EA value is plotted in Figure 1. Likewise, for the fluorinated cubanes, C<sub>8</sub>H<sub>8-n</sub>F<sub>n</sub>, there are three isomers for *n* = 2, 3, 5, and 6 and six isomers for *n* = 4. Only the isomers with the highest EAs are plotted in Figure 1. The spin densities for the radical anions of perfluorocyclopropane and perfluorocubane are shown in Figure 2.

There are too many isomers to consider the complete hydrofluorocarbon series corresponding to cyclobutane, cyclopentane, cyclohexane, bicyclo[1.1.1]pentane, bicyclo[2.2.2]octane, adamantane, and dodecahedrane. For each of these interesting frameworks, calculations are reported here only for selected degrees of fluorination. The results are included in Table 2 (or, for negative EA values, in the Supporting Information), and spin densities for selected radical anions are plotted in Figure 2.

In some cases (noted in the tables), the geometry of the radical anion is less symmetric than that of the corresponding neutral molecule. This may be an artifact reflecting the lack of electron correlation in the UHF/6-31+G(d) geometry calculation. For example, the UHF structure for the perfluoroadamantane radical anion (C<sub>10</sub>F<sub>16</sub><sup>-</sup>) has C<sub>3v</sub> symmetry, while density functional theory (DFT) calculations yield a symmetrical T<sub>d</sub> structure.<sup>21</sup> Such geometric distortions are not expected to affect the general trends in electron affinities. However, they may distort the spin densities substantially. For example, for C<sub>10</sub>F<sub>16</sub><sup>-</sup> the B3LYP spin density at the UHF geometry is localized in the stretched tertiary C–F bond, in contrast with the symmetric B3LYP/6-31+G(d) structure plotted in Figure 2. Likewise, for the perfluorocyclohexane radical anion, the UHF structure has one long C–F bond, but the B3LYP structure (shown in Figure 2) is symmetrical.

Scheme 1 implies that the added electron will be inside the carbon cage. A reviewer suggested, instead, that it is outside the box, delocalized on the fluorine atoms. The plots in Figure 2 display the spin density ( $\rho_{\text{spin}} \equiv \rho_{\alpha} - \rho_{\beta}$ ). Plots of the SOMO ( $\phi_{\text{SOMO}}$ ), or of the density difference between the anionic and the neutral molecules ( $\Delta\rho = \rho_{\text{anion}} - \rho_{\text{neutral}}$ ), look similar. To provide quantitative measures,  $\rho_{\text{spin}}$ ,  $\rho_{\text{SOMO}} = \phi_{\text{SOMO}}^2$ , and  $\Delta\rho$  were integrated over the interior of the carbon cages of perfluorinated tetrahedrane, cubane, adamantane, and dodecahedrane. The results are listed in Table 3. In each case, the integral over all space equals 1, so the tabulated quantity can be considered as the fraction of the added electron that is inside the box. For each molecule, the interior integrals of  $\rho_{\text{spin}}$  and  $\rho_{\text{SOMO}}$  are nearly equal, as expected, and are larger than the integral of  $\Delta\rho$ . However, all of the integrals indicate that the electron is mostly outside the carbon cage. To measure how much of the added charge resides on the fluorine atoms, a natural population analysis (NPA) was performed.<sup>22</sup> The differences in atomic populations between the anionic and the neutral molecules are included in Table 3. The carbon and fluorine atoms absorb comparable amounts of the added charge, tending more toward the fluorine atoms as the cage becomes larger. In adamantane, the tertiary (3°) positions absorb most of the charge, as suggested by the plot of  $\rho_{\text{spin}}$  shown in Figure 2.

## Discussion

**Cages.** In cage molecules, the component  $\sigma^*$  orbitals radiate from the center in three dimensions. The best examples considered here are the platonic molecules tetrahedrane, cubane, and dodecahedrane. In these molecules all of the carbon centers are tertiary, which is the most favorable situation. The importance of the tertiary C–F centers has been emphasized by Paul et al. in their studies of perfluoroalkanes<sup>3</sup> and of perfluorinated methylcycloalkanes.<sup>9</sup> The extra electron occupies a delocalized, totally symmetric orbital (Figure 2). The additional C–C bonding causes the cage to contract slightly in the radical anion

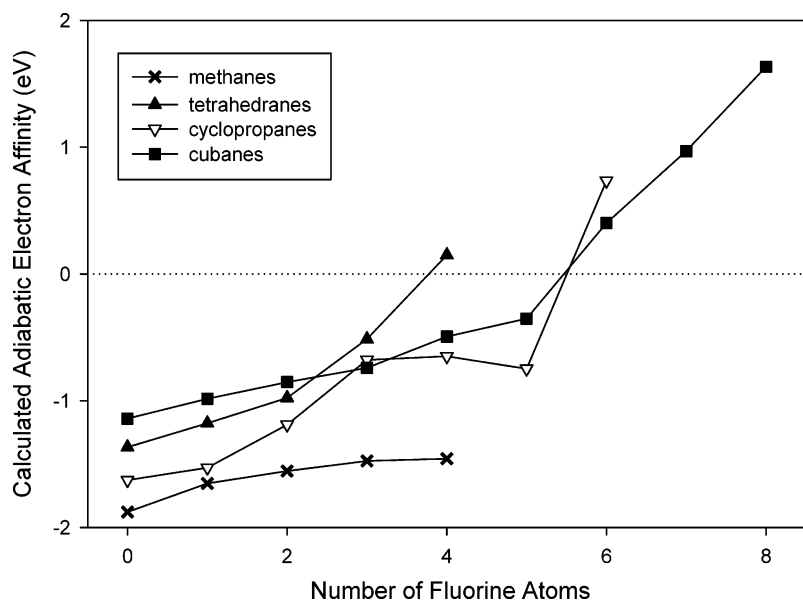


Figure 1. Computed electron affinities of some hydrofluorocarbon series.

TABLE 2: Summary of Selected Computational Results<sup>a</sup>

molecule <sup>b</sup>	point group <sup>c</sup>	ZPE (kJ mol <sup>-1</sup> )	anion ZPE (kJ mol <sup>-1</sup> )	neutral $E_c$ (hartree)	anion $E_c$ (hartree)	EA (eV)
tetrahedrane (C <sub>4</sub> H <sub>4</sub> )	$T_d$	155.0	156.9	-154.643746	-154.594245	-1.37
tetrafluorotetrahedrane	$T_d$	81.6	78.4	-551.492977	-551.497237	0.15
cubane (C <sub>8</sub> H <sub>8</sub> )	$O_h$	346.8	345.2	-309.466157	-309.423596	-1.14
<i>o</i> -hexafluorocubane	$C_{2v}$	226.8	215.3	-904.893650	-904.904034	0.40
<i>m</i> -hexafluorocubane	$C_{2v}$	226.6	216.8	-904.896439	-904.901930	0.25
<i>p</i> -hexafluorocubane	$D_{3d}(C_1)$	226.4	224.8	-904.899076	-904.889634	-0.24
heptafluorocubane	$C_{3v}$	203.9	194.5	-1004.123055	-1004.155053	0.97
octafluorocubane	$O_h$	186.6	174.6	-1103.347470	-1103.402906	1.63
dodecahedrane (C <sub>20</sub> H <sub>20</sub> )	$I_h(C_i)$	926.6	902.8	-774.195332	-774.160657	-0.70
icosafafluorododecahedrane	$I_h$	502.1	496.4	-2758.850893	-2758.985771	3.73
adamantane (C <sub>10</sub> H <sub>16</sub> )	$T_d$	626.5	623.7	-390.732136	-390.694152	-1.00
hexadecafluoroadamantane	$T_d(C_{3v})$	296.5	285.3	-1978.516190	-1978.565714	1.46
hexafluorocyclopropane (C <sub>3</sub> F <sub>6</sub> )	$D_{3h}$	91.5	74.8	-713.302051	-713.322730	0.74
octafluorocyclobutane (C <sub>4</sub> F <sub>8</sub> )	$D_{2d}(D_{4h})$	127.1	110.3	-951.138052	-951.172375	1.11
decafluorocyclopentane (C <sub>5</sub> F <sub>10</sub> )	$C_2(D_{5h})$	161.8	145.6	-1188.953243	-1188.987890	1.11
dodecafluorocyclohexane (C <sub>6</sub> F <sub>12</sub> )	$D_{3d}(C_1)$	195.0	182.4	-1426.751129	-1426.774654	0.77

<sup>a</sup> Equilibrium electronic energies (B3LYP/6-31+G(d)//HF/6-31+G(d)) are labeled  $E_c$ . <sup>b</sup> Among isomers, boldface indicates the isomer with the highest calculated EA value. See the Supporting Information for molecular structures. <sup>c</sup> HF/6-31+G(d) level; anion point group in parentheses if different.

relative to the neutral molecule; the calculated C–C distances across the cage are 1.473 Å in C<sub>4</sub>F<sub>4</sub>, 1.465 Å in C<sub>4</sub>F<sub>4</sub><sup>-</sup>, 2.700 Å in C<sub>8</sub>F<sub>8</sub>, 2.674 Å in C<sub>8</sub>F<sub>8</sub><sup>-</sup>, 4.353 Å in C<sub>20</sub>F<sub>20</sub>, and 4.326 Å in C<sub>20</sub>F<sub>20</sub><sup>-</sup>. Complementarily, because the caged orbital is composed of C–F antibonding orbitals, the C–F bonds lengthen upon electron attachment by 0.017 Å in C<sub>4</sub>F<sub>4</sub>, 0.034 Å in C<sub>8</sub>F<sub>8</sub>, and 0.017 Å in C<sub>20</sub>F<sub>20</sub>.

The EAs of partially fluorinated cubanes depend upon the choice of isomer (Table 2 and Supporting Information). This may be understood in terms of overlap among individual (i.e., valence-bond-type) C–F  $\sigma^*$  orbitals. For example, for tetrafluorocubane the tetrahedral arrangement of fluorine atoms yields a calculated EA approximately equal to that for the parent hydrocarbon. But placing all four fluorine atoms on a single face of the cube increases the calculated EA by 0.64 eV. An even larger disparity is found for hexafluorocubane. If the two hydrogen atoms are on opposite vertices of the cube, then the calculated EA is 0.90 eV greater than that for C<sub>8</sub>H<sub>8</sub>. Moving them to adjacent vertices raises the EA by an additional 0.64 eV. A similar argument, in terms of overlap between neighboring CF<sub>2</sub> fragment orbitals, has been invoked to rationalize the characteristic  $\pi$ -bonding in perfluorocycloalkane radical anions.<sup>23</sup>

After correcting for the bias indicated in Table 1 (by subtracting 0.33 eV), the present calculations suggest that the platonic fluorocarbon molecules have electron affinities of zero (C<sub>4</sub>F<sub>4</sub>), 1.30 ± 0.14 eV (C<sub>8</sub>F<sub>8</sub>), and 3.40 ± 0.14 eV (C<sub>20</sub>F<sub>20</sub>). The value for perfluorododecahedrane is remarkably high, equal to that for atomic fluorine.<sup>4</sup> Introducing secondary carbon centers has a surprising effect on the electron affinity. Despite having twice as many fluorine atoms as perfluorotetrahedrane, the calculated EA for perfluorobicyclo[1.1.1]pentane is 0.41 eV lower. Decreasing the ring strain and adding six more fluorine atoms, to produce perfluorobicyclo[2.2.2]octane, provides almost no increase in calculated EA. Plots of radical anion spin density (not shown) show localization on the axis between the tertiary carbon atoms.

Perfluoroadamantane (C<sub>10</sub>F<sub>16</sub>) has been the subject of extensive DFT calculations.<sup>21</sup> It contains four tertiary and six secondary carbon centers. After correcting for bias, the EA is predicted here to be 1.13 ± 0.14 eV. This is somewhat lower than the value of 1.31 eV predicted by Li et al.<sup>21</sup> Regardless of the precise value, it is larger than that typical for linear fluorocarbons<sup>3</sup> and much larger than that of the parent hydrocarbon (by 2.47 eV in the present calculations). As shown in Figure 2, the spin density is delocalized among the tertiary C–F

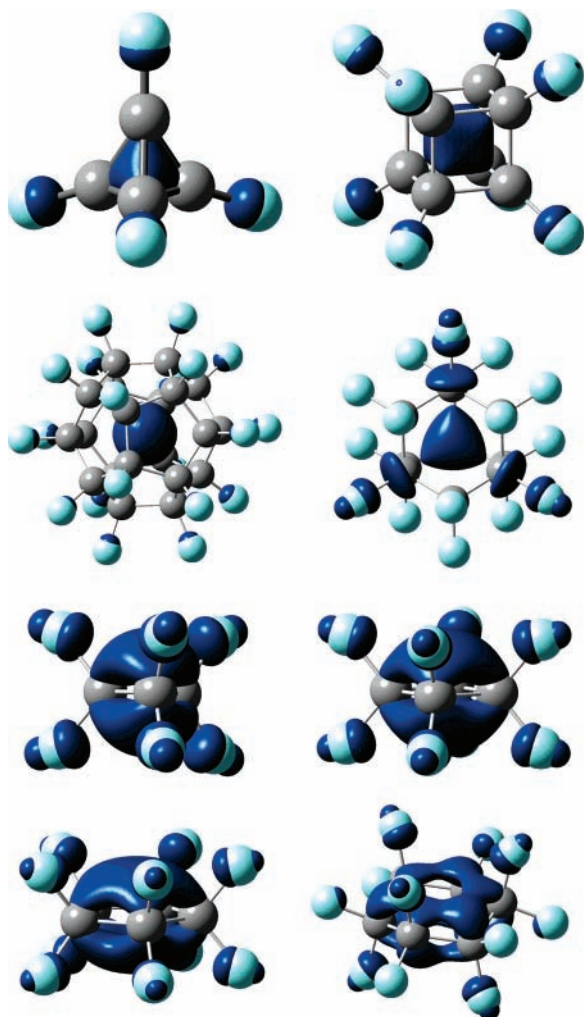


**Figure 2.** B3LYP spin densities (contour = 0.005) in perfluorinated radical anions of tetrahedrane and cubane (first row), dodecahedrane and adamantane (second row), cyclopropane and cyclobutane (third row), and cyclopentane and cyclohexane (fourth row).

**TABLE 3: Selected Densities<sup>a</sup> Integrated over Cage Interiors and Changes in Atomic Charges upon Electron Attachment**

molecule	$\rho_{\text{spin}}$	$\rho_{\text{SOMO}}$	$\Delta\rho$	$\Delta q_{\text{C}}$	$\Delta q_{\text{F}}$
C <sub>4</sub> F <sub>4</sub>	0.026	0.024	0.019	-0.183	-0.067
C <sub>8</sub> F <sub>8</sub>	0.110	0.113	0.047	-0.063	-0.062
C <sub>10</sub> F <sub>16</sub>	0.170	0.184	0.064	-0.105 (3°)	-0.076 (3°)
				-0.009 (2°)	-0.018 (2°)
C <sub>20</sub> F <sub>20</sub>	0.350	0.350	0.049	-0.017	-0.033

<sup>a</sup>  $\rho_{\text{spin}}$  = spin density;  $\rho_{\text{SOMO}}$  = square of the singly occupied (highest  $\alpha$ -spin) orbital;  $\Delta\rho$  = difference between the total densities of the anion and the neutral species (at the anionic geometry).

bonds and in the center of the cage. This and the small changes in atomic charges (Table 3) suggest that the secondary carbon centers (i.e., CF<sub>2</sub> groups) are merely spectators. However, when *only* the four tertiary centers are fluorinated (*tet*-tetrafluoroadamantane, C<sub>10</sub>H<sub>12</sub>F<sub>4</sub>) the calculated EA is only 0.02 eV greater than that for the parent C<sub>10</sub>H<sub>16</sub>. In the complementary case, if only the secondary carbons are fluorinated (*tet*-dodecafluoroadamantane, C<sub>10</sub>H<sub>4</sub>F<sub>12</sub>), then the computed EA is also about the same as that in the parent hydrocarbon. Thus, there is a dramatic cooperative effect achieved by complete fluorination. In the cubanes, the EA is maximized for isomers with the closest arrangement of fluorine substituents. This may be mimicked in adamantane by fluorinating one tertiary carbon and the three

vicinal secondary carbons to generate *vic*-heptafluoroadamantane, C<sub>10</sub>H<sub>9</sub>F<sub>7</sub>. The EA of this molecule is 0.50 eV greater than that of *tet*-dodecafluoroadamantane despite having fewer fluorine atoms. Fluorinating the distal methylene groups instead (generating *p*-heptafluoroadamantane) yields an EA 0.30 eV lower than that for the vicinal isomer.

**Rings.** It has long been known that cyclic fluorocarbons are more electron-attracting than linear analogues.<sup>24</sup> Perfluorocyclobutane is the most studied in this series, and its EA is known experimentally, by thermal detachment equilibrium measurements, to be 0.63 ± 0.05 eV.<sup>25</sup> Gallup<sup>26</sup> appears to have been the first to notice the unusual characteristics of the corresponding radical anions. His calculations showed that perfluorocyclobutane, which has the expected puckered structure, becomes flattened upon attaching an electron. This is consistent with earlier electron spin resonance (ESR) spectra that revealed all of the fluorine atoms to be equivalent in the radical anions.<sup>27</sup> Surprisingly, the added electron occupies an orbital that has a node in the plane of the carbon framework. The planar, delocalized  $\pi$  structure has been confirmed convincingly, using a combination of experimental and theoretical ESR spectra, for the series *c*-C<sub>3</sub>F<sub>6</sub>, *c*-C<sub>4</sub>F<sub>8</sub>, and *c*-C<sub>5</sub>F<sub>10</sub>.<sup>23,28</sup> Changes in C–C and C–F distances upon electron attachment, as found in the present and previous calculations,<sup>9,23,26,28</sup> are consistent with the description of the extra orbital as C–C  $\pi$ -bonding and C–F  $\sigma$ -antibonding. A DFT study revealed that *c*-C<sub>6</sub>F<sub>12</sub> and *c*-C<sub>7</sub>F<sub>14</sub> do not share this behavior and predicted EA values of 0.24, 0.70, 0.77, 0.40, and 0.40 eV, respectively, for *c*-C<sub>*n*</sub>F<sub>2*n*</sub> (*n* = 3–7).<sup>9</sup> The present values are comparable: 0.41, 0.78, 0.78, and 0.44 eV for *n* = 3–6 (all with estimated standard uncertainty  $\sigma$  = 0.14 eV). The corresponding spin densities are shown in Figure 2.

Just as for the cubanes, the EAs of partially fluorinated cycloalkanes depend upon the choice of isomer. For example, the calculated EA of *cis*-1,2,3-trifluorocyclopropane is 0.49 eV greater than that for 1,1,2-trifluorocyclopropane. The singly occupied molecular orbital (SOMO) is a  $\pi$  orbital as for the perfluorinated molecule. However, the lobe of the  $\pi$  orbital near the fluorine atoms is smaller than the distal lobe, as expected from the electronic crowding effect described in the Introduction. An analogous result is obtained for *cis*-1,2,3,4-tetrafluorocyclobutane. (The calculated EA is 0.71 eV greater than that for the all-*trans* isomer.) Fluorinating the other face of the molecule further stabilizes the  $\pi$  molecular orbital.

**Electronic Structure.** To rationalize the enhanced electron affinities of cyclic fluorocarbons, Mittal and Libby described these molecules as “intramolecular electrostatic trap(s) for electrons”.<sup>29</sup> Curiously, they presented their electrostatic model as “more general” than the molecular orbital (MO) model. Because they apparently believed that the MO model did not apply to cyclic fluorocarbons, it is ironic that their summary of the MO model describes Scheme 1 so well: “It is deduced that compounds in which atoms are suitably disposed to afford the maximum overlap of vacant orbitals should constitute suitable electron acceptors so that a stable reduced species might be obtained.” A similar electrostatic description, based upon alignment of strong C–F bond dipoles, was suggested by Gallup.<sup>26</sup> However, no electrostatic model explains why the added electron in *c*-C<sub>*n*</sub>F<sub>2*n*</sub> (*n* = 3–5) occupies a  $\pi$  orbital instead of a  $\sigma$  orbital.

In a study using K-shell energy-loss spectroscopy, Ishii et al. observed the enhanced stability of the lowest unoccupied molecular orbital (LUMO) in cyclic fluorocarbons.<sup>30</sup> They assigned the LUMO as C–C  $\sigma^*$ , with ring strain stabilizing

**TABLE 4: EA Ratios: Comparison of Electrostatic<sup>29</sup> and Molecular Orbital<sup>31</sup> Model Predictions with the Present Calculations**

denominator molecule	numerator molecule	elect.	MO	calcd. <sup>a</sup>
1 <i>H</i> ,1 <i>H</i> -hexafluorocyclobutane	octafluorocyclobutane	1.3	2.0	5.4
1 <i>H</i> ,4 <i>H</i> -decafluorobicyclo[2.2.1]heptane	1 <i>H</i> -undecafluorobicyclo[2.2.1]heptane	1.1	1.8	2.3
1 <i>H</i> ,4 <i>H</i> -decafluorobicyclo[2.2.1]heptane	dodecafluorobicyclo[2.2.1]heptane	1.2	2.6	6.9
<i>trans</i> -tetrafluorocyclobutane	<i>cis</i> -tetrafluorocyclobutane	1.0	>3	2.6
<i>up,up,down,down</i> -tetrafluorocyclobutane	<i>cis</i> -tetrafluorocyclobutane	1.0	>2	1.3
<i>cis</i> -tetrafluorocyclobutane	octafluorocyclobutane	2.0	2.0	2.3
<i>tet</i> -tetrafluorocubane	<i>fac</i> -tetrafluorocubane	1.0	∞	54
<i>p</i> -hexafluorocubane	<i>o</i> -hexafluorocubane	1.0	1.1	1.7
<i>tet</i> -tetrafluoroadamantane	hexadecafluoroadamantane	4.0	∞	121
<i>tet</i> -tetrafluoroadamantane	<i>tet</i> -dodecafluoroadamantane	3.0	∞	-0.2 <sup>b</sup>
<i>p</i> -heptafluoroadamantane	<i>vic</i> -heptafluoroadamantane	1.0	>3	2.6

<sup>a</sup> To obtain a comparable number, the calculated ratio is  $\Delta EA_2/\Delta EA_1$ , where  $\Delta EA$  is relative to the parent hydrocarbon. <sup>b</sup> Both values of  $\Delta EA$  are near zero.

the C–C antibonding orbitals (and destabilizing the C–C bonding orbitals). However, they had some difficulty reconciling this assignment with the absence of the distinctive features in the spectra of equally strained hydrocarbons and with the persistence of the features in spectra of unstrained *c*-C<sub>5</sub>F<sub>10</sub> and *c*-C<sub>6</sub>F<sub>12</sub>. Their minimal-basis ab initio calculations on *c*-C<sub>3</sub>F<sub>6</sub> were the first to show the  $\pi$ -type LUMO ( $a_2''$ ), but the authors discounted that result, presumably not trusting such a counter-intuitive result from such a crude calculation.

The electrostatic model by Mittal and Libby has been critiqued effectively by Liebman, who presented a molecular orbital model instead.<sup>31</sup> He considered each CF<sub>2</sub> fragment as having a lowest unoccupied fragment orbital (LUFO; not his terminology) of the  $\sigma^*$  type, that is, with negative phase on both fluorine atoms and positive phase on the carbon atom. An eclipsed arrangement of adjacent CF<sub>2</sub> groups has more favorable overlap between the respective LUFOs, leading to a more delocalized and stable molecular orbital (LUMO). The degree of stabilization could be estimated simply by counting eclipsed 1,2 and 1,3 F–F interactions. Liebman presented some predictions for comparison with the electrostatic model by Mittal and Libby. Table 4 lists those and other predictions of the two models for relative EAs. Theoretical values from the present study are also provided. However, because most of the molecules do not bind an electron at all, the theoretical ratios in Table 4 are between values of  $\Delta EA$ , defined here as the calculated EA relative to that for the parent hydrocarbon. All computed EA values are from Table 2 or the Supporting Information. Liebman's molecular orbital model is better than the electrostatic model except for the prediction involving *up,up,down,down*-tetrafluorocyclobutane. Both models fail to predict that tetrahedral tetrafluoro- and dodecafluoroadamantane have nearly equal EA values.

All of the qualitative models fail to predict the  $\pi$  symmetry of the negative ion. As suggested by ElSohly et al.,<sup>23</sup> Liebman's model can accommodate the  $\pi$  character if the CF<sub>2</sub> LUFO is considered to be the  $\pi$ -type combination of the C–F  $\sigma^*$  orbitals ( $b_2$  representation in local  $C_{2v}$  symmetry) instead of the  $\sigma$ -type combination ( $a_1$ ). This is reasonable because each C–F  $\sigma^*$  orbital has a node (nearly) in the carbocyclic plane. The orbital phase will moderate vicinal interactions in this  $\pi$  molecular orbital. For the comparisons in Table 4, this leads to slightly worse predictions than the original model because it predicts no interaction between adjacent CF and CF<sub>2</sub> groups in adamantanes, because their LUFOs are orthogonal. A further modification, to employ  $a_1$  orbitals only when more favorable than the corresponding  $b_2$  orbitals, is no better than Liebman's original MO model for the comparisons in Table 4. However, it does reproduce the  $\pi$  character of the cyclic radical anions.

**Potential Extensions and Applications.** Interesting generalizations and applications of sigma stellation can be envisioned. Scheme 1 illustrates how a starlike arrangement of vacant molecular orbitals facilitates formation of a negative ion (n-type stellation). A similar arrangement of lone-pair orbitals will facilitate the formation of a positive ion (p-type stellation). Such molecules are known. For example, ionization energies below 7 eV have been predicted<sup>32</sup> and measured<sup>33</sup> for adamantanes (tricyclic bridgehead tetramines). The sigma-delocalized electronic structure has been verified (by using magnetic spectroscopies) for cage-like polyamine radical cations.<sup>34–36</sup>

Cyclic fluorocarbons have attracted interest partly because of their propensity to form charge-transfer complexes.<sup>6,37</sup> A solid solution of n-type and p-type stellated molecules is expected to be either a charge-transfer salt or a small-band-gap material. Because charge transfer creates unpaired electrons, such materials may have interesting magneto-optical properties. Alternatively, n- or p-type molecules might be useful as dopants in organic semiconductors.

Because the radical anions of cyclic fluorocarbons are  $\pi$  systems, stacking them could lead to linear, noncovalent electron delocalization perpendicular to the carbocyclic planes. Intercalation between aromatic rings may have a similar effect. Covalently bonded oligomers and polymers of cage molecules such as perfluorocubane may have extensively delocalized negative-ion states whose character could be tuned by choosing different monomer(s) or chain lengths. Their physical properties would probably be similar to those of polytetrafluoroethylene. Some monomers, such as perfluorocyclobutane, undergo a conformational change upon electron attachment. There could be an abrupt, cooperative change in geometry when a corresponding oligomer is reduced strongly enough.

## Conclusions

Positional isomers of partially fluorinated cyclic hydrocarbons have widely varying electron affinities. This can be understood in terms of overlap between individual C–F  $\sigma^*$  orbitals, which is strongest for vicinal isomers. The same principle applies to cage compounds, with the additional feature of orbital overlap inside the cage. Tertiary C–F  $\sigma^*$  orbitals are more stable than secondary orbitals. Interesting properties are expected for analogous radical cations, for polymers of (poly)cyclic fluorocarbons, and for noncovalent complexes or materials.

**Note Added in Proof.** For C<sub>20</sub>F<sub>20</sub>, Zhang, Wu, and Jiao recently reported EA = 3.66 eV, based upon B3LYP/6-311+G(d)/B3LYP/6-31G(d) calculations.<sup>38</sup> Their paper includes plots of the HOMO and LUMO of C<sub>20</sub>F<sub>20</sub>, an analysis of aromaticity, and the energetics of several endohedral complexes

with atoms and atomic anions. This followed more approximate calculations, including endohedral atomic dianions, by Zhang and Wu.<sup>39</sup> I regret not learning earlier of their prior work.

**Supporting Information Available:** Structures illustrating nomenclature, a version of Table 2 including more molecules, and HF/6-31+G(d) optimized geometries, energies, vibrational frequencies, and infrared intensities. This material is available free of charge via the Internet at <http://pubs.acs.org>.

## References and Notes

- (1) Spyrou, S. M.; Sauer, I.; Christophorou, L. G. *J. Chem. Phys.* **1983**, *78*, 7200–7216.
- (2) Gutsev, G. L.; Adamowicz, L. *J. Chem. Phys.* **1995**, *102*, 9309–9314.
- (3) Paul, A.; Wannere, C. S.; Schaefer, H. F., III. *J. Phys. Chem. A* **2004**, *108*, 9428–9434.
- (4) Bartmess, J. E. In *NIST Chemistry WebBook*; Linstrom, P. J., Mallard, W. G., Eds.; National Institute of Standards and Technology: Gaithersburg, MD, 2005.
- (5) Hughes, R. P.; LeHusebo, T.; Maddock, S. M.; Rheingold, A. L.; Guzei, I. A. *J. Am. Chem. Soc.* **1997**, *119*, 10231–10232.
- (6) Burdeniuc, J.; Sanford, M.; Crabtree, R. H. *J. Fluorine Chem.* **1998**, *91*, 49–54.
- (7) Combellas, C.; Kanoufi, F.; Thiébaud, A. *J. Phys. Chem. B* **2003**, *107*, 10894–10905.
- (8) Koch, E. C. *Propellants, Explos., Pyrotech.* **2004**, *29*, 9–18.
- (9) Paul, A.; Wannere, C. S.; Kasalova, V.; Schleyer, P. v. R.; Schaefer, H. F., III. *J. Am. Chem. Soc.* **2005**, *127*, 15457–15469.
- (10) Scott, A. P.; Radom, L. *J. Phys. Chem.* **1996**, *100*, 16502–16513.
- (11) Becke, A. D. *J. Chem. Phys.* **1993**, *98*, 5648–5652.
- (12) Stephens, P. J.; Devlin, F. J.; Chabalowski, C. F.; Frisch, M. J. *J. Phys. Chem.* **1994**, *98*, 11623–11627.
- (13) Lee, C.; Yang, W.; Parr, R. G. *Phys. Rev. B* **1988**, *37*, 785–789.
- (14) Certain commercial materials and equipment are identified in this paper to specify procedures completely. In no case does such identification imply recommendation or endorsement by the National Institute of Standards and Technology, nor does it imply that the material or equipment identified is necessarily the best available for the purpose.
- (15) Frisch, M. J.; Trucks, G. W.; Schlegel, H. B.; Scuseria, G. E.; Robb, M. A.; Cheeseman, J. R.; Zakrzewski, V. G.; Montgomery, J. A., Jr.; Stratmann, R. E.; Burant, J. C.; Dapprich, S.; Millam, J. M.; Daniels, A. D.; Kudin, K. N.; Strain, M. C.; Farkas, O.; Tomasi, J.; Barone, V.; Cossi, M.; Cammi, R.; Mennucci, B.; Pomelli, C.; Adamo, C.; Clifford, S.; Ochterski, J.; Petersson, G. A.; Ayala, P. Y.; Cui, Q.; Morokuma, K.; Malick, D. K.; Rabuck, A. D.; Raghavachari, K.; Foresman, J. B.; Cioslowski, J.; Ortiz, J. V.; Stefanov, B. B.; Liu, G.; Liashenko, A.; Piskorz, P.; Komaromi, I.; Gomperts, R.; Martin, R. L.; Fox, D. J.; Keith, T.; Al-Laham, M. A.; Peng, C. Y.; Nanayakkara, A.; Gonzalez, C.; Challacombe, M.; Gill, P. M. W.; Johnson, B. G.; Chen, W.; Wong, M. W.; Andres, J. L.; Head-Gordon, M.; Replogle, E. S.; Pople, J. A. *Gaussian 98*; Gaussian, Inc.: Pittsburgh, PA, 1998.
- (16) Frisch, M. J.; Trucks, G. W.; Schlegel, H. B.; Scuseria, G. E.; Robb, M. A.; Cheeseman, J. R.; Montgomery, J. A., Jr.; Vreven, T.; Kudin, K. N.; Burant, J. C.; Millam, J. M.; Iyengar, S. S.; Tomasi, J.; Barone, V.; Mennucci, B.; Cossi, M.; Scalmani, G.; Rega, N.; Petersson, G. A.; Nakatsuji, H.; Hada, M.; Ehara, M.; Toyota, K.; Fukuda, R.; Hasegawa, J.; Ishida, M.; Nakajima, T.; Honda, Y.; Kitao, O.; Nakai, H.; Klene, M.; Li, X.; Knox, J. E.; Hratchian, H. P.; Cross, J. B.; Bakken, V.; Adamo, C.; Jaramillo, J.; Gomperts, R.; Stratmann, R. E.; Yazyev, O.; Austin, A. J.; Cammi, R.; Pomelli, C.; Ochterski, J. W.; Ayala, P. Y.; Morokuma, K.; Voth, G. A.; Salvador, P.; Dannenberg, J. J.; Zakrzewski, V. G.; Dapprich, S.; Daniels, A. D.; Strain, M. C.; Farkas, O.; Malick, D. K.; Rabuck, A. D.; Raghavachari, K.; Foresman, J. B.; Ortiz, J. V.; Cui, Q.; Baboul, A. G.; Clifford, S.; Cioslowski, J.; Stefanov, B. B.; Liu, G.; Liashenko, A.; Piskorz, P.; Komaromi, I.; Martin, R. L.; Fox, D. J.; Keith, T.; Al-Laham, M. A.; Peng, C. Y.; Nanayakkara, A.; Challacombe, M.; Gill, P. M. W.; Johnson, B.; Chen, W.; Wong, M. W.; Gonzalez, C.; Pople, J. A. *Gaussian 03*; Gaussian, Inc.: Wallingford, CT, 2003.
- (17) Ervin, K. M. *Chem. Rev.* **2001**, *101*, 391–444.
- (18) Ervin, K. M. *Chem. Rev.* **2002**, *102*, 855–855.
- (19) Rienstra-Kiracofe, J. C.; Tschumper, G. S.; Schaefer, H. F., III.; Nandi, S.; Ellison, G. B. *Chem. Rev.* **2002**, *102*, 231–282.
- (20) Berdys, J.; Anusiewicz, I.; Skurski, P.; Simons, J. *J. Am. Chem. Soc.* **2004**, *126*, 6441–6447.
- (21) Li, Q.-S.; Feng, X.-J.; Xie, Y.; Schaefer, H. F., III. *J. Phys. Chem. A* **2005**, *109*, 1454–1457.
- (22) Reed, A. E.; Weinstock, R. B.; Weinhold, F. *J. Chem. Phys.* **1985**, *83*, 735–746.
- (23) ElSohly, A. M.; Tschumper, G. S.; Crocombe, R. A.; Wang, J. T.; Williams, F. *J. Am. Chem. Soc.* **2005**, *127*, 10573–10583.
- (24) Rajbenbach, L. A. *J. Am. Chem. Soc.* **1966**, *88*, 4275–4277.
- (25) Miller, T. M.; Friedman, J. F.; Viggiano, A. A. *J. Chem. Phys.* **2004**, *120*, 7024–7028.
- (26) Gallup, G. A. *Chem. Phys. Lett.* **2004**, *399*, 206–209.
- (27) Hasegawa, A.; Shiotani, M.; Williams, F. *Faraday Discuss.* **1977**, *63*, 157–174.
- (28) Shiotani, M.; Lund, A.; Lunell, S.; Williams, F. *J. Phys. Chem. A* **2007**, *111*, 321–338.
- (29) Mittal, J. P.; Libby, W. F. *Nature* **1968**, *220*, 1027–1028.
- (30) Ishii, I.; McLaren, R.; Hitchcock, A. P. *Can. J. Chem.* **1988**, *66*, 2104–2121.
- (31) Liebman, J. F. *J. Fluorine Chem.* **1973**, *3*, 27–33.
- (32) Galasso, V. *Chem. Phys.* **2001**, *270*, 79–91.
- (33) He, Y. G.; Wu, C. Y.; Kong, W.; Schultz, K. P.; Nelsen, S. F. *J. Phys. Chem. A* **2005**, *109*, 959–961.
- (34) Kirste, B.; Alder, R. W.; Sessions, R. B.; Bock, M.; Kurreck, H.; Nelsen, S. F. *J. Am. Chem. Soc.* **1985**, *107*, 2635–2640.
- (35) Gerson, F.; Gescheidt, G.; Knöbel, J.; Martin, W. B., Jr.; Neumann, L.; Vogel, E. *J. Am. Chem. Soc.* **1992**, *114*, 7107–7115.
- (36) Zwier, J. M.; Brouwer, A. M.; Keszthelyi, T.; Balakrishnan, G.; Offersgaard, J. F.; Wilbrandt, R.; Barbosa, F.; Buser, U.; Amaudrut, J.; Gescheidt, G.; Nelsen, S. F.; Little, C. D. *J. Am. Chem. Soc.* **2002**, *124*, 159–167.
- (37) Hammond, P. R. *J. Chem. Phys.* **1971**, *55*, 3468–3471.
- (38) Zhang, C.-Y.; Wu, H.-S.; Jiao, H. *J. Mol. Model.* **2007**, *13*, 499–503.
- (39) Zhang, C.-Y.; Wu, H.-S. *Theochem—J. Mol. Struct.* **2007**, *815*, 71–74.